ARTICLE

Z_3 Charge Density Wave of Silicon Atomic Chains on a Vicinal Silicon Surface

Euihwan Do, Jae Whan Park, Oleksandr Stetsovych, Pavel Jelinek, and Han Woong Yeom*

Read Online

ACCESS | Metrics & More | Article Recommendations | Supporting Information

ABSTRACT: An ideal one-dimensional electronic system is formed along atomic chains on Au-decorated vicinal silicon surfaces, but the nature of its low-temperature phases has been puzzling for last two decades. Here, we unambiguously identify the low-temperature structural distortion of this surface using high-resolution atomic force microscopy and scanning tunneling microscopy. The most important structural ingredient of this surface, the step-edge Si chains, are found to be strongly buckled, every third atom down, forming trimer unit cells. This observation is consistent with the recent model of rehybridized dangling bonds and rules out the antiferromagnetic spin ordering proposed earlier. The spectroscopy and electronic structure calculation indicate a charge density wave insulator with a Z_3 topology, making it possible to exploit topological phases and excitations. The tunneling current was found to substantially lower the energy barrier between three degenerate CDW states, which induces a dynamically fluctuating CDW at very low temperature.

KEYWORDS: *topological soliton, charge density wave, atomic wire, scanning tunneling microscopy, atomic force microscopy, density functional theory*
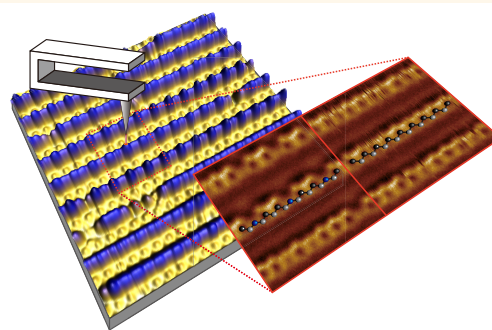
INTRODUCTION

One-dimensional (1D) electronic systems have attracted great research interest due to their simplicity with exactly solvable models, the exploded manifestation of many-body interactions, and topological properties. Non-Fermi liquid behaviors,[1,2] charge/spin density wave phenomena,[3−5] nontrivial topology,[6] and topological excitations[7] are among notable issues discussed actively. While bulk compounds with strongly anisotropic structures and organic crystals[8] have been widely investigated materials hosting 1D electronic systems, self-assembled[6,7,9−16] or atom-manipulated[17,18] atomic chain structures on solid surfaces are in the spotlight recently. As notable examples of self-assembled atomic chains, charge density wave (CDW) and a new type of solitons were discussed in indium chain structures on silicon surfaces,[6,7] non-Fermi liquid behaviors[10−12] and quantum spin chains[13−15] in gold-induced chains on silicon surfaces, and Majorana edge modes in iron chain structures on a lead surface.[16]

Among those representative atomic chain systems, Au-induced atomic chain structures on stepped Si surfaces have remained puzzling with intriguing phase transitions of elusive origin.[10−15,19−23] The stepped surface of Si(553) with submonolayer Au deposited has been known to feature well ordered atomic chain arrays, which are composed basically of

Au atomic rows embedded into the topmost Si layer and honeycomb Si chains formed along its step edges (Figure 1a).[13−15,24] The latter provides chains of Si dangling bonds localized on step edges. These atomic chains were discovered to exhibit two different symmetry-broken structures at low temperature; ×2 and ×3 orderings on terrace Au and step-edge Si chains, respectively ($2a_0$ and $3a_0$ with $a_0 = 0.384$ nm, the Si lattice constant along steps). Origins of the superstructures have been controversial for a long time.[13−15,21,22,25−28] The recent electron diffraction study revealed that the ×2 structure along the terrace Au chains has a static structural distortion without a drastic temperature dependence,[25,27] which is consistently supported by the recent density functional theory (DFT) calculations.[15] However, the origin of the temperature-induced ×3 ordering along Si step-edge chains[21,29] is still unclear with the suggestions of the electronic/structural instability[15,26,28] and the antiferromagnetic spin ordering on
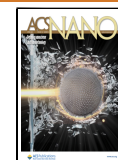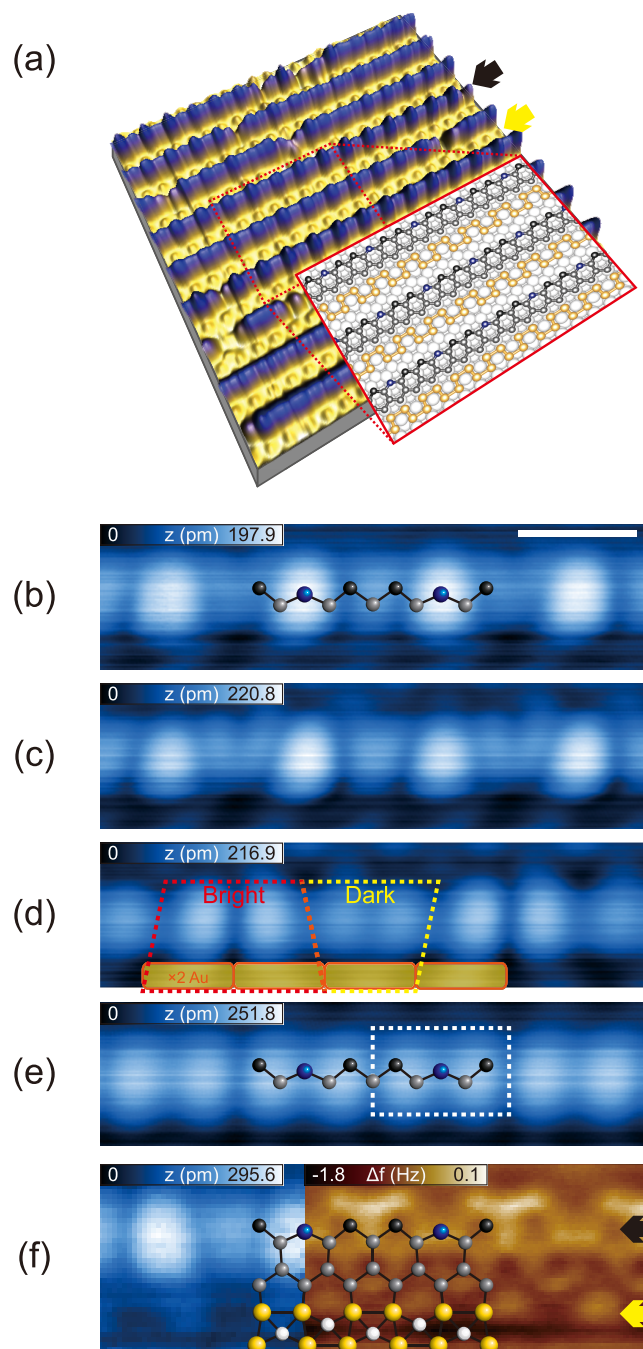
Figure 1. (a) Topographic STM image (13.6 × 13.6 nm^2 at +0.9 V sample bias) of Si(553)-Au at 50 K and schematics of the rehybridized model.[15] Si (Au) atoms are represented by small (large) spheres. High-resolution (b,c) empty- and (d,e) filled-state STM images (at V = +0.9, + 0.4, −0.4, and −0.7 V, respectively, with I = 10 pA) for four unit cells of the ×3 step-edge chain. The scale bar in (b) corresponds to 1.0 nm. (f) Comparison between 50 K STM (V = +0.9 V and I = 5 pA) and 4.3 K AFM (V = 0 V) images resolving clearly step-edge Si (black arrow) and terrace Au (yellow) chains.

Si dangling bonds.[13] On the basis of the latter, even a quantum spin liquid phase was suggested.[14,25] Namely, there exist two lines of models, which are distinctly based on charge/structural and spin degrees of freedom, respectively. Moreover, making the investigation of the ground state more challenging, the apparent structure along Si step-edge chains in scanning tunneling microscopy (STM) changes into another ×2 ordering below about 60 K.[30,31] The atomic structure of this ordering is not clear at all but was suggested to be induced by the tunneling current.[30,32] This means that STM cannot probe the pristine ground state at low temperature.

In the present work, we report an atomic resolution noncontact (nc) atomic force microscopy (AFM) study on the Si(553)-Au surface together with simultaneous STM measurements. These combined measurements provide effective decoupling of the possible excitation source (tunneling current) and the local structural probe (AFM). The unperturbed step-edge Si structure at 4.3 K is observed to possess a trimer ground state with every third atom distorted downward and with an insulating property. This clearly rules out the spin ordering model[13,14] and supports strongly the charge/structure-modulated model.[15] The present model

corresponds to a CDW ground state with a triple degeneracy or a Z_3 topology for the Si step-edge chain,[21,22,33] whose electronic states are unexpectedly decoupled from those of neighboring Au chains. The tunneling current injection is found to induce an apparently undistorted structure in AFM but a buckled dimer structure in STM. This structure is explained by the fluctuation between three translationally degenerate trimer structures with their translational barrier reduced substantially by the tunneling current. The present work thus solves a long-standing puzzle on the structure of this model 1D electronic system. Beyond that, this work discloses the topological nature of the present system and introduces it as a platform for manipulating topological phases and topological excitations such as Z_3 solitons. The combination of atomic resolution STM and AFM can be widely applied to decouple not only the electronic modulation from atomic structure but also the electronic local excitation source for manipulation from the structural probe.

RESULTS AND DISCUSSION

Figure 1 panels b and e show the well-known empty- and filled-state STM images taken at 50 K along a step edge of the Si(553)-Au surface, respectively. The brightest protrusions in the STM images are due to Si step-edge atoms (Figure 1f). At this temperature, the perturbation by the tunneling current[30,31] is not substantial and the step edge exhibits the well-known ×3 superstructure.[13−15] On the other hand, the atomic chains on narrow terraces show a ×2 superstructure with a much reduced contrast (indicated by a yellow arrow in Figure 1f). These results are fully consistent with many previous STM works.[14,21,29−31,35,36] Note also the strong bias dependence of the STM images (Figure 1b−e), which indicates a substantial electronic effect for these images such as the spin splitting[13,14] or the rehybridization of dangling bonds.[15]

In stark contrast, a Δf image of nc-AFM can reveal directly the structural distortion, if any, since it sensitively detects the relative distance between the tip and individual surface atoms. The corresponding image of Figure 1f exhibits a strong negative Δf (the dark contrast in the image), which indicates surface atoms closer to the tip. This image tells immediately that the step edge is structurally distorted with a significant height difference. Since the height (contrast) of the two (black) atoms are similar to those of the terrace atoms, we can conclude that every third (blue) atoms of the step edge has a downward distortion. We also observe the alternating bright and dark contrast in a ×2 period along the Au chains within the narrow terraces between Si step edges in the AFM image (pointed by the yellow arrow), which is consistent with what is observed in the STM images. Since the Au atomic positions would be represented by dark contrast, this image indicates a dimerlike pairing of Au atoms. The former is crucial for the debate on the surface structure since the recent structure models share the double Au row structure with a ×2 distortion along the terrace but differ substantially in the structural distortion on the Si step edge.[13−15,24] Namely, the previous calculations and the present one indicate that the structural distortion of the antiferromagnetic spin chain model is negligible, in clear contrast to the present AFM observation even though this model gives a strong electronic modulation in STM similar to that of the rehybridized model. On the other hand, the strong step-edge distortion revealed in the nc-AFM image is consistent with the rehybridized step-edge chain model (Figure 1f).[13−15] Furthermore, the atomic origin of the

STM protrusions can be disclosed unambiguously by the high-resolution Δf image of the same structure taken simultaneously with STM. The strong empty-state protrusion is localized on the down-distorted Si atom at the step edge and the double protrusions in the filled state on the undistorted Si atoms. This is fully consistent with the result of the DFT calculations based on the reconstruction of step-edge Si atoms within the rehybridization model.[15] This reconstruction, the downward distortion on every third atoms, splits the sp_3 dangling bond into sp_2 and p orbitals in filled and empty states, respectively, which explains the corresponding STM contrast.[15]

The reconstruction of step-edge atoms would be reflected in surface electronic states. Figure 2 panels a and b show the band
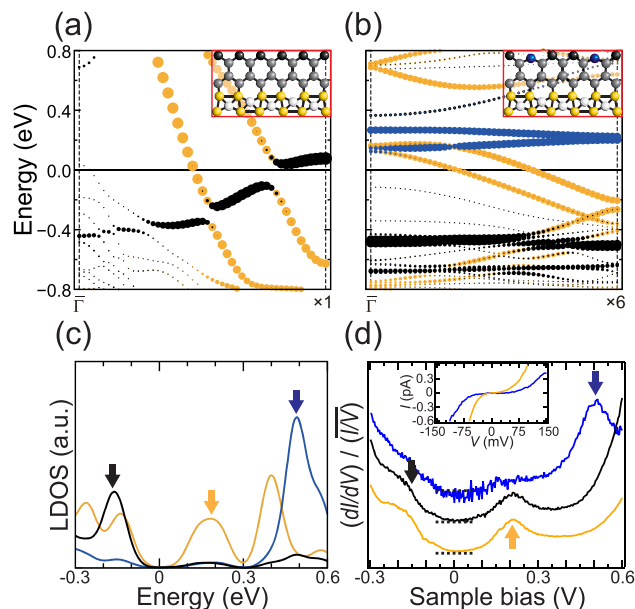
Figure 2. Calculated band structures of (a) undistorted and (b) distorted surfaces along the step-edge direction. The insets show the schematics of the structure models, respectively. (c) Calculated and (d) measured local density of states (LDOS) spectra on the step-edge Si chain (blue and black for distorted and undistorted atoms, respectively) and on the terrace Au chain (yellow). For the calculated spectra, the energy is shifted for +0.3 eV for comparison. The dI/dV spectra are normalized conductance (the method described in ref 34) and were measured at 50 K to prevent the unintended current-induced transition. Curves are vertically offset for comparison (dashed lines indicate zeros). Five prominent spectral features are specified on the curves (blue, black, and yellow arrows). Inset: I−V curves recorded from ×3 step-edge Si (blue) and terrace Au (yellow) chains. In comparison with the calculated LDOS, one has to consider a roughly parabolic background in the experiment centered at zero bias.

structures calculated along step edges. In the undistorted structure (Figure 2a), the Au chains have two strongly metallic bands coming from the double Au rows consistent with the previous angle-resolved photoemission measurements.[21,23] Note that the spin−orbit coupling is not included here, which explains small extra splittings observed in these Au 6s bands.[23] The silicon dangling bonds along step edges also form a metallic band. This is naturally expected from the partially filled nature of dangling bonds. The Au and Si bands are hybridized, and the latter receives electrons from the substrate to be filled over the half filling. As mentioned above, the step-
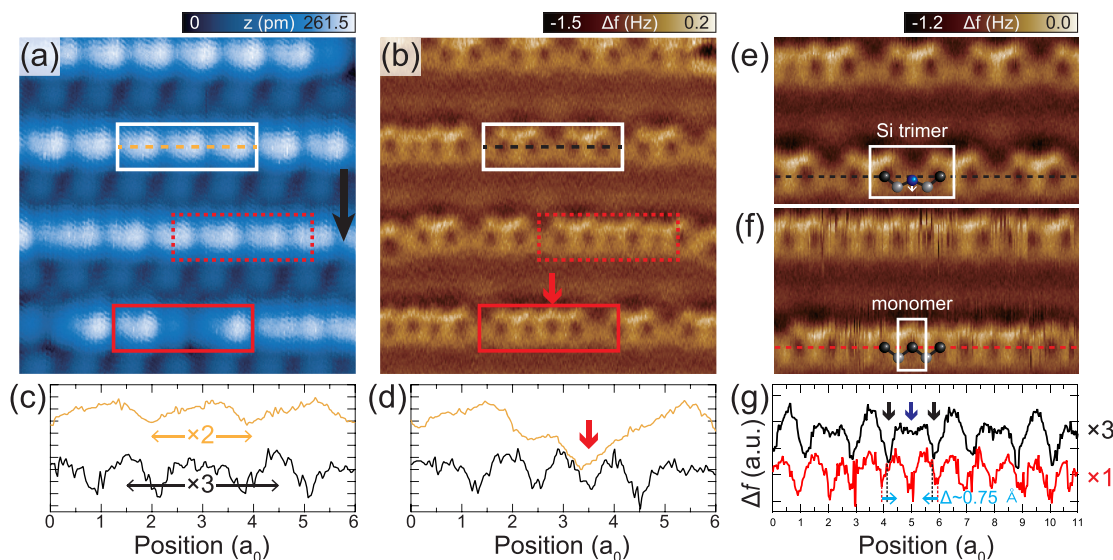
Figure 3. Topographic (a) STM and (b) AFM images (5.6×5.6 nm^2) of Si(553)-Au at 4.3 K. The images are taken at +1.0 (STM, with I = 10 pA) and 0 (AFM) sample biases. The black arrow indicates the uphill direction of the steps. Comparison of STM (yellow) and AFM (black) line profiles taken across the (c) Si step-edge wire (white rectangle) and (d) static adsorbate impurity[29] (solid red). Bias-dependent AFM images measured at (e) 0 and (f) +0.5 V sample biases. (g) Δf line profiles taken across the Si step-edge chain at 0 (black) and +0.5 V (red), which exhibit two different surface states of trimer and monomer, respectively. The down-distorted (undistorted) atom of the trimer structure is represented by blue (black) sphere.

edge reconstruction splits the Si band into the empty p band just above the Fermi level and the fully filled sp$_2$ band (blue and black circles in Figure 2b, respectively). These states are rather well localized on the distorted and undistorted Si atoms, respectively. The ×2 distortion on the Au chains also makes a band gap, but it is located above the Fermi level around +0.4 eV. Thus, the Au chains keep its metallic property but the Si chains become insulating with a gap larger than 0.6 eV. These calculated results explain the main features of the measured STS (dI/dV) spectra (Figure 2d). Most importantly, the density of states for Si chains of the reconstructed surface exhibit a substantial splitting of the main spectra with the strong localization of the empty-state feature (+0.50 eV) on the distorted atom (the blue arrow) and the filled state (−0.16 eV) on the undistorted atoms (the black arrow). The empty state closer to the Fermi level at +0.2 eV is due to the electronic state related to Au chains. This state appears also in the spectra of the Si chain atoms, which seems to indicate the limited spatial resolution of this particular STS measurement. The insulating property of the Si chains can be clearly deduced from the STS measurements in contrast to the Au chains (inset of Figure 2d and see Figure S1 in the Supporting Information for more the detailed gap measurements). The major discrepancy between the calculation and the measurement is the rigid shift of the spectra by 0.3 eV (Figure 2c,d), which obviously indicates a less charge transfer from the Si substrate than calculated. A smaller charge transfer (or a hole doping) puts the Fermi level of the Si step-edge chain well within its band gap. Within this situation, namely with the large band gap formation and the shift of the Fermi level for the Si dangling-bond band, the insulating property of the Si step-edge chain becomes robust, and the coupling of the bands of Si and Au chains becomes much less significant. In our additional calculations, we prove that the mild hole doping indeed leads to a rigid shift of the Si states and is favorable for the ×3 CDW formation on the step-edge Si (Figure S2 in the

Supporting Information). In contrast, the electron doping suppresses the ×3 structure, which will be discussed below.

The distorted and insulating Si step-edge chains straightforwardly indicate a CDW insulator although its mechanism is largely different from most known CDW systems. The mechanism is not fully consistent with the Fermi surface nesting of a dispersive band but is much closer to the Jahn–Teller distortion. However, the present band gap is not a bonding–antibonding splitting of the Jahn–Teller effect but an orbital rehybridization or the orbital ordering of p and sp$_2$ orbitals. Since the distortion has a ×3 periodicity, there exist three degenerate ground states. This corresponds to a realization of a Z_3 topological insulator, whose material realization has not been reported to our best knowledge. Topological excitations or solitons of this system are expected to have fractional charges of $(2/3)$e and $(4/3)$e.[33,37,38] The soliton excitation of the present system was suggested in an early STM work for local defects[22] and in the recent electron diffraction study for the thermally induced disordering,[25,26,29] and was identified experimentally very recently.[39] The present structural information provides a solid ground for the existence of such exotic topological solitons.

As mentioned above, the STM images at lower temperature were reported to exhibit different superstructures, developing gradually a new ×2 superstructure.[30,31] Figure 3a shows an empty-state STM image recorded at 4.3 K where the effect of tunneling current was reported to dominate. It is apparent that both chains have a $2a_0$ periodicity with Si step-edge atoms in apparent up-and-down buckling contrast. However, at the same temperature and position, the nc-AFM image shows mainly the ×3 superstructure (Figures 3b,c), which is consistent with the measurements at 50 K. Thus, we can ensure that the ×2 structure on the step edge is indeed induced by tunneling current as suggested in the previous works.[30,31] The effect of the tunneling current can further be corroborated by the nc-AFM measurement with the tunneling current on;
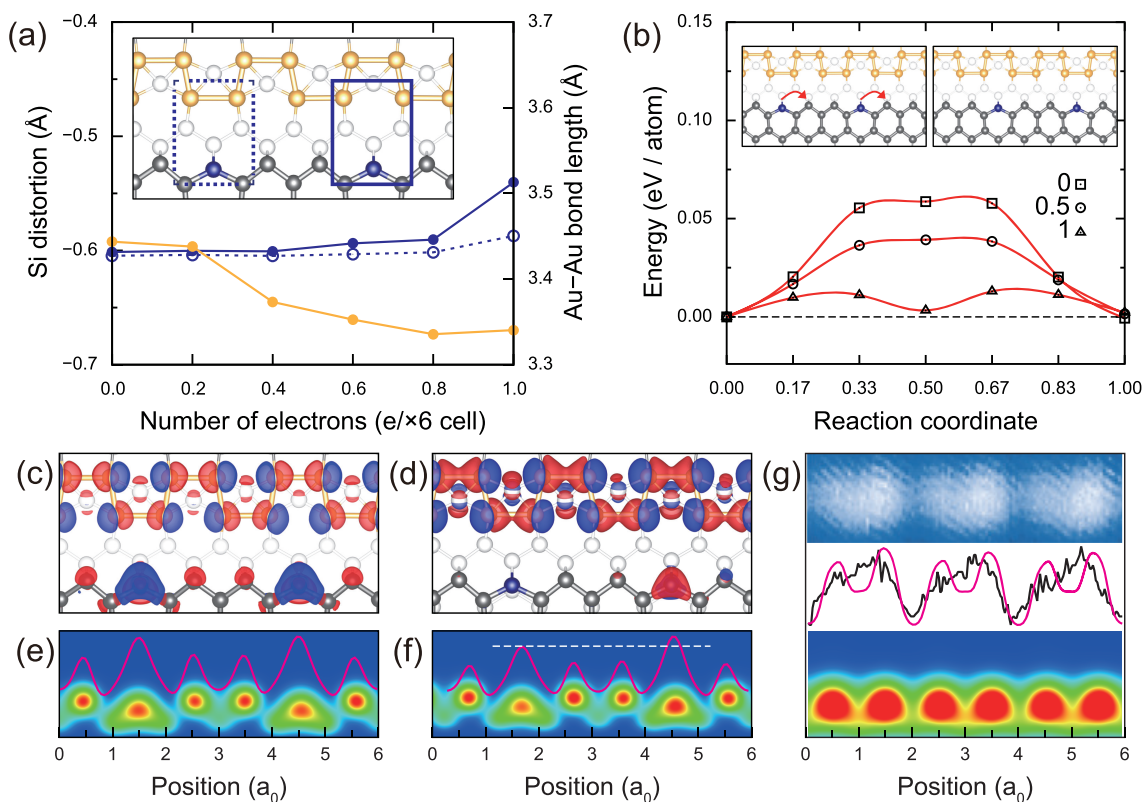
Figure 4. Electron doping effect on a CDW ground state of the Si(553)-Au surface. (a) Structural distortions of the Si step-edge chain (blue) and the Au terrace chain (yellow) as a function of electron doping. Inset: solid and dashed rectangles indicate the distorted Si atoms placed close to the long and the short Au−Au bonds, respectively. (b) Translational energy barriers between the degenerate ground states for different electron doping levels. Inset: initial and final states for a diffusion process. (c,d) Isosurface of total charge difference ($\Delta\rho$). (c) $\Delta\rho = \rho_{CDW} - \rho_{\times 1}$ (7×10^{-3} e Å^{-3}) for the undoped surface ($\rho_{0.0}$). (d) $\Delta\rho = \rho_{1.0} - \rho_{0.0}$ (2×10^{-3} e Å^{-3}). Red (blue) color indicates positive (negative) charges. Simulated STM images ($V = +1.0$ V and $z = 2$ Å) for (e) undoped and (f) doped (1.0e) ×6 supercells. Magenta lines indicate z profiles along the step-edge chain. (g) Comparison between the STM image at 4.3 K (top) and the simulated one ($V = +1.0$ V and $z = 4$ Å) averaged for all three degenerate ground states (bottom).

while the AFM images shown so far are obtained with the null tip bias (Figure 3e), we can also obtain the same quality image with the tunneling current (bias of 0.5 V) (Figure 3f). Figure 3 panels e−g unambiguously indicate that the trimer reconstruction on the step edge is completely relieved by the tunneling current and the current-induced transition was observed to be reversible (Figure S3). This confirms that the ground-state reconstruction is based on the ×3 and ×2 superstructures along the Si step-edge and Au terrace chains, respectively. In fact, the apparently undistorted structure is observed locally in the AFM image without the tunneling current in Figure 3b (dashed rectangle), which is thought to be due to the presence of local defects.

The origin of this additional structure with a weak buckling in the STM image can be explained by the electron doping effect within our theoretical calculations. The transient electron doping by tunneling current was already proposed to explain the tunneling-induced structure within the antiferromagnetic spin chain model.[30,31] This model suggested that a $2a_0$-periodic antiferromagnetic spin ordering is favored over the $3a_0$ one when the system is doped. This model, however, cannot explain the much reduced STM contrast in the ×2 superstructure as compared with that of ×3, since the ×2 and ×3 antiferromagnetic orderings of spins produce the same amount of exchange splitting and electronic modulation. In Figure 4, the structural and electronic properties of the

surface were examined for various electron doping levels by using the present rehybridized model.[15] The additional electron doping enhances the Au−Au bond length to form a stronger ×2 distortion of the Au chain (Figure 4a), which is consistent with the previous theoretical study.[40] In stark contrast, the doping relieves the distortion of Si step-edge atoms to suppress the ×3 CDW order, especially after the saturation of the Au dimerization around 0.8e doping. This indicates that doped electrons fill the metallic Au bands (Figures 2b and 4c) at the initial stage and, at a higher doping level, accumulate on the unoccupied part of the distorted Si bands to destabilize the distorted structure (Figure 4c,d). As a result, the energy gain of the ×3 CDW structure is significantly reduced together with the transition energy barrier between three translationally degenerate ×3 structures (Figure 4b). Since three degenerate ground states compete each other with a small energy barrier of 13 meV, at a finite temperature, the doped system would exhibit a dynamic fluctuation between them. The averaged STM image over three degenerate states matches excellently with the weakly buckled ×2 structure observed by STM at low temperature (Figure 4g). The weak buckling is the effect of the strong Au dimerization, which affects the translational potential energy between the degenerate states (see the Supporting Information Figure S4).

CONCLUSIONS

The atomic and electronic structures of the Si(553)-Au chain system are investigated by atomic resolution nc-AFM together with simultaneous STM/STS measurements. These measurements unambiguously reveal the strong trimer structural distortion and a substantial band gap along the step-edge Si chains at low temperature, which corresponds to a CDW ground state and a Z_3 topological insulator. The transient electron doping by the tunneling current is shown to reduce the stability of the CDW phase to induce a dynamically fluctuating CDW state at very low temperature. Further studies on topological properties and topological excitations in this system are thus highly promising. In particular, the exploitation of the Z_3 topological solitons in the present system would provide opportunity for the topologically protected multilevel information processing. The combination of atomic resolution STM and AFM is shown to be useful to decouple the electronic local excitation source for manipulation from the structural probe.

METHODS

Atomically resolved imaging and spectroscopy of the Si(553)-Au surface were performed by simultaneous high-resolution nc-AFM and STM measurements under ultrahigh vacuum at two different temperatures of 4.3 and 50 K using a commercial low-temperature microscope (SPECS GmbH) with force−current detection capabilities. A tungsten tip mounted on a tuning fork was used for both AFM and STM measurements. AFM images were obtained by measuring the frequency shift (Δf) of the tuning fork at constant height mode. For scanning tunneling spectroscopy (STS) measurements, current−voltage ($I−V$) curves were recorded with the lock-in technique using a modulation amplitude of 10 mV. The clean Si(553) surface was prepared by repeated flash heating to 1520 K. Gold was evaporated onto the clean Si(553) surface held at 923 K. At a Au coverage of around 0.5 monolayer, well-ordered Si(553)-Au surfaces were reproducibly fabricated.[29,36] DFT calculations were performed using the Vienna ab initio simulation package[41] within the generalized-gradient approximation (GGA) using the revised Perdew−Burke−Ernzerhof (PBEsol) functional.[42] The Si(553)-Au surface is modeled within periodic supercells with six bulklike Si layers and a vacuum spacing of about 12.8 Å. The bottom of the slab was passivated by H atoms. We used a plane-wave basis with an energy cutoff of 312 eV and $5 \times 2 \times 1$ k-point mesh. All atoms but the bottom two Si layers were relaxed until the residual force components were within 0.03 eV/Å.

ASSOCIATED CONTENT

Ⓢ Supporting Information

The Supporting Information is available free of charge at https://pubs.acs.org/doi/10.1021/acsnano.2c00972.

Further discussion on the quantitative estimation of the band gap (Figure S1), the stability of the CDW phase upon doping (Figure S2), the reversibility of the current-induced transition (Figure S3), and the STM image simulation for the current(doping)-induced structure (Figure S4) (PDF)

AUTHOR INFORMATION

Corresponding Author

Han Woong Yeom − Center for Artificial Low Dimensional Electronic Systems, Institute for Basic Science (IBS), Pohang 37673, Republic of Korea; Department of Physics, Pohang University of Science and Technology (POSTECH), Pohang 37673, Republic of Korea; orcid.org/0000-0002-8538-8993; Email: yeom@postech.ac.kr

Authors

Euihwan Do − Center for Artificial Low Dimensional Electronic Systems, Institute for Basic Science (IBS), Pohang 37673, Republic of Korea; Department of Physics, Pohang University of Science and Technology (POSTECH), Pohang 37673, Republic of Korea

Jae Whan Park − Center for Artificial Low Dimensional Electronic Systems, Institute for Basic Science (IBS), Pohang 37673, Republic of Korea

Oleksandr Stetsovych − Institute of Physics of the Czech Academy of Sciences, 18221 Prague, Czech Republic

Pavel Jelinek − Institute of Physics of the Czech Academy of Sciences, 18221 Prague, Czech Republic; orcid.org/0000-0002-5645-8542

Complete contact information is available at:
https://pubs.acs.org/10.1021/acsnano.2c00972

Author Contributions

E.D. performed STM and AFM experiments and analyzed data. J.W.P. performed DFT and model calculations. O.S. and P.J. helped AFM experiments. H.W.Y. conceived the project idea and directed experiments/calculations. E.D., J.W.P., and H.W.Y. wrote the manuscript. E.D. and J.W.P. equally contributed to this work.

Notes

The authors declare no competing financial interest.

REFERENCES

(1) Auslaender, O. M.; Yacoby, A.; de Picciotto, R.; Baldwin, K. W.; Pfeiffer, L. N.; West, K. W. Tunneling Spectroscopy of the Elementary Excitations in a One-Dimensional Wire. Science 2002, 295, 825−828.

(2) Ishii, H.; Kataura, H.; Shiozawa, H.; Yoshioka, H.; Otsubo, H.; Takayama, Y.; Miyahara, T.; Suzuki, S.; Achiba, Y.; Nakatake, M.; et al. Direct observation of Tomonaga−Luttinger-liquid state in carbon nanotubes at low temperatures. Nature 2003, 426, 540−544.

(3) Yeom, H. W.; Takeda, S.; Rotenberg, E.; Matsuda, I.; Horikoshi, K.; Schaefer, J.; Lee, C. M.; Kevan, S. D.; Ohta, T.; Nagao, T.; Hasegawa, S. Instability and Charge Density Wave of Metallic Quantum Chains on a Silicon Surface. Phys. Rev. Lett. 1999, 82, 4898−4901.

(4) Zeng, C.; Kent, P.; Kim, T.-H.; Li, A.-P.; Weitering, H. H. Charge-order fluctuations in one-dimensional silicides. Nat. Mater. 2008, 7, 539−542.

(5) Schlappa, J.; et al. Spin−orbital separation in the quasi-one-dimensional Mott insulator Sr_2CuO_3. Nature 2012, 485, 82−85.

(6) Cheon, S.; Kim, T.-H.; Lee, S.-H.; Yeom, H. W. Chiral solitons in a coupled double Peierls chain. Science 2015, 350, 182−185.

(7) Kim, T.-H.; Cheon, S.; Yeom, H. W. Switching chiral solitons for algebraic operation of topological quaternary digits. Nat. Phys. 2017, 13, 444−447.

(8) Island, J. O.; Molina-Mendoza, A. J.; Barawi, M.; Biele, R.; Flores, E.; Clamagirand, J. M.; Ares, J. R.; Sánchez, C.; van der Zant, H. S. J.; D'Agosta, R.; Ferrer, I. J.; Castellanos-Gomez, A. Electronics and optoelectronics of quasi-1D layered transition metal trichalcogenides. 2D Materials 2017, 4, 022003.

(9) Do, E. H.; Yeom, H. W. Electron Quantization in Broken Atomic Wires. *Phys. Rev. Lett.* **2015**, *115*, 266803.

(10) Segovia, P.; Purdie, D.; Hengsberger, M.; Baer, Y. Observation of spin and charge collective modes in one-dimensional metallic chains. *Nature* **1999**, *402*, 504−507.

(11) Losio, R.; Altmann, K. N.; Kirakosian, A.; Lin, J.-L.; Petrovykh, D. Y.; Himpsel, F. J. Band Splitting for Si(557)-Au: Is It Spin-Charge Separation? *Phys. Rev. Lett.* **2001**, *86*, 4632−4635.

(12) Ahn, J. R.; Yeom, H. W.; Yoon, H. S.; Lyo, I.-W. Metal-Insulator Transition in Au Atomic Chains on Si with Two Proximal Bands. *Phys. Rev. Lett.* **2003**, *91*, 196403.

(13) Erwin, S. C.; Himpsel, F. J. Intrinsic magnetism at silicon surfaces. *Nat. Commun.* **2010**, *1*, 58.

(14) Hafke, B.; Frigge, T.; Witte, T.; Krenzer, B.; Aulbach, J.; Schäfer, J.; Claessen, R.; Erwin, S. C.; Horn-von Hoegen, M. Two-dimensional interaction of spin chains in the Si(553)-Au nanowire system. *Phys. Rev. B* **2016**, *94*, 161403.

(15) Braun, C.; Gerstmann, U.; Schmidt, W. G. Spin pairing versus spin chains at Si(553)-Au surfaces. *Phys. Rev. B* **2018**, *98*, 121402.

(16) Nadj-Perge, S.; Drozdov, I. K.; Li, J.; Chen, H.; Jeon, S.; Seo, J.; MacDonald, A. H.; Bernevig, B. A.; Yazdani, A. Observation of Majorana fermions in ferromagnetic atomic chains on a super-conductor. *Science* **2014**, *346*, 602−607.

(17) Fölsch, S.; Martinez-Blanco, J.; Yang, J.; Kanisawa, K.; Erwin, S. C. Quantum dots with single-atom precision. *Nat. Nanotechnol.* **2014**, *9*, 505−508.

(18) Drost, R.; Ojanen, T.; Harju, A.; Liljeroth, P. Topological states in engineered atomic lattices. *Nat. Phys.* **2017**, *13*, 668−671.

(19) Crain, J. N.; Kirakosian, A.; Altmann, K. N.; Bromberger, C.; Erwin, S. C.; McChesney, J. L.; Lin, J.-L.; Himpsel, F. J. Fractional Band Filling in an Atomic Chain Structure. *Phys. Rev. Lett.* **2003**, *90*, 176805.

(20) Crain, J. N.; McChesney, J. L.; Zheng, F.; Gallagher, M. C.; Snijders, P. C.; Bissen, M.; Gundelach, C.; Erwin, S. C.; Himpsel, F. J. Chains of gold atoms with tailored electronic states. *Phys. Rev. B* **2004**, *69*, 125401.

(21) Ahn, J. R.; Kang, P. G.; Ryang, K. D.; Yeom, H. W. Coexistence of Two Different Peierls Distortions within an Atomic Scale Wire: Si(553)-Au. *Phys. Rev. Lett.* **2005**, *95*, 196402.

(22) Snijders, P. C.; Rogge, S.; Weitering, H. H. Competing Periodicities in Fractionally Filled One-Dimensional Bands. *Phys. Rev. Lett.* **2006**, *96*, 076801.

(23) Yeom, H. W.; Jung, S. W.; Shin, J. S.; Kim, J.; Kim, K. S.; Miyamoto, K.; Okuda, T.; Namatame, H.; Kimura, A.; Taniguchi, M. Direct observation of the spin polarization in Au atomic wires on Si(553). *New J. Phys.* **2014**, *16*, 093030.

(24) Krawiec, M. Structural model of the Au-induced Si(553) surface: Double Au rows. *Phys. Rev. B* **2010**, *81*, 115436.

(25) Hafke, B.; Brand, C.; Witte, T.; Sothmann, B.; Horn-von Hoegen, M.; Erwin, S. C. Thermally Induced Crossover from 2D to 1D Behavior in an Array of Atomic Wires: Silicon Dangling-Bond Solitons in Si(553)-Au. *Phys. Rev. Lett.* **2020**, *124*, 016102.

(26) Braun, C.; Neufeld, S.; Gerstmann, U.; Sanna, S.; Plaickner, J.; Speiser, E.; Esser, N.; Schmidt, W. G. Vibration-Driven Self-Doping of Dangling-Bond Wires on Si(553)-Au Surfaces. *Phys. Rev. Lett.* **2020**, *124*, 146802.

(27) Edler, F.; Miccoli, I.; Pfnür, H.; Tegenkamp, C. Charge-transfer transition in Au-induced quantum wires on Si(553). *Phys. Rev. B* **2019**, *100*, 045419.

(28) Plaickner, J.; Speiser, E.; Braun, C.; Schmidt, W. G.; Esser, N.; Sanna, S. Surface localized phonon modes at the Si(553)-Au nanowire system. *Phys. Rev. B* **2021**, *103*, 115441.

(29) Shin, J. S.; Ryang, K.-D.; Yeom, H. W. Finite-length charge-density waves on terminated atomic wires. *Phys. Rev. B* **2012**, *85*, 073401.

(30) Polei, S.; Snijders, P. C.; Erwin, S. C.; Himpsel, F. J.; Meiwes-Broer, K.-H.; Barke, I. Structural Transition in Atomic Chains Driven by Transient Doping. *Phys. Rev. Lett.* **2013**, *111*, 156801.

(31) Polei, S.; Snijders, P. C.; Meiwes-Broer, K.-H.; Barke, I. Current-dependent periodicities of Si(553)-Au. *Phys. Rev. B* **2014**, *89*, 205420.

(32) Brihuega, I.; Custance, O.; Ugeda, M. M.; Oyabu, N.; Morita, S.; Gómez-Rodríguez, J. M. Direct Observation of a (3×3) Phase in α-Pb/Ge(111) at 10 K. *Phys. Rev. Lett.* **2005**, *95*, 206102.

(33) Liu, X.; Agarwal, G. S. The New Phases due to Symmetry Protected Piecewise Berry Phases; Enhanced Pumping and Non-reciprocity in Trimer Lattices. *Sci. Rep.* **2017**, *7*, 45015.

(34) Feenstra, R. M. Tunneling spectroscopy of the (110) surface of direct-gap III-V semiconductors. *Phys. Rev. B* **1994**, *50*, 4561−4570.

(35) Aulbach, J.; Schäfer, J.; Erwin, S. C.; Meyer, S.; Loho, C.; Settelein, J.; Claessen, R. Evidence for Long-Range Spin Order Instead of a Peierls Transition in Si(553)-Au Chains. *Phys. Rev. Lett.* **2013**, *111*, 137203.

(36) Aulbach, J.; Erwin, S. C.; Kemmer, J.; Bode, M.; Schäfer, J.; Claessen, R. Parity breaking in a double atomic chain system. *Phys. Rev. B* **2017**, *96*, 081406.

(37) Su, W. P.; Schrieffer, J. R.; Heeger, A. J. Solitons in Polyacetylene. *Phys. Rev. Lett.* **1979**, *42*, 1698−1701.

(38) Su, W. P.; Schrieffer, J. R.; Heeger, A. J. Soliton excitations in polyacetylene. *Phys. Rev. B* **1980**, *22*, 2099−2111.

(39) Park, J. W.; Do, E.; Shin, J. S.; Song, S. K.; Stetsovych, O.; Jelinek, P.; Yeom, H. W. Creation and annihilation of mobile fractional solitons in atomic chains. *Nat. Nanotechnol.* **2022**, *17*, 244−249.

(40) Mamiyev, Z.; Sanna, S.; Lichtenstein, T.; Tegenkamp, C.; Pfnür, H. Extrinsic doping on the atomic scale: Tuning metallicity in atomic Au chains. *Phys. Rev. B* **2018**, *98*, 245414.

(41) Kresse, G.; Furthmüller, J. Efficient iterative schemes for ab initio total-energy calculations using a plane-wave basis set. *Phys. Rev. B* **1996**, *54*, 11169−11186.

(42) Perdew, J. P.; Ruzsinszky, A.; Csonka, G. I.; Vydrov, O. A.; Scuseria, G. E.; Constantin, L. A.; Zhou, X.; Burke, K. Restoring the Density-Gradient Expansion for Exchange in Solids and Surfaces. *Phys. Rev. Lett.* **2008**, *100*, 136406.